Journal of the European Ceramic Society **17** (1997) 191–196

PII: S0955-2219(96)00157-4
0955-2219/97/$17.00

Rheological Behaviour of a Polymer Ceramic Blend

M. Dubus & H. Burlet

Ecole Nationale Supérieure de Mines de Paris, Centre des Matériaux, BP 91003 Evry Cedex, France

(Received 15 September 1995; accepted 23 July 1996)

Abstract

The rheological behaviour of an alumina injection moulding suspension was studied. A capillary rheometer allowing working under accurate injection moulding conditions has been developed. The main result concerns the observed slip phenomenon. It was shown that wall slip is reinforced with higher temperatures and decreasing shear rates. An attempt was made to correlate the results of the rheological study with the emergence of injection moulding defects. Normal filling was observed at low temperature, but solid jetting appeared under high temperatures and low shear rates. This unusual behaviour is a consequence of the wall slip mechanism. At low temperatures, when no slip was detected on rheological measurement, a steady front flow takes place. At higher temperatures, wall slip is favoured to shearing and unsteady front flow is obtained. © *1996 Published by Elsevier Science Limited.*

1 Introduction

Powder injection moulding is a technology able to produce a new range of components from powders. A major attraction is the economical production of complex parts materials. The process involves several steps, from mixing to sintering, but the production of reliable shapes requires correct injection moulding conditions. This paper reports a study performed to correlate the rheological behaviour of an alumina binder compound, measured in a rheometer, with the moulding behaviour. The goal is to optimize the process conditions in order to produce defects-free parts. Such a correlation has often been used for unfilled thermoplastics but has not been addressed for highly filled polymers. A blend composed of a commercial powder and a polystyrene-based binder was chosen.

2 Experimental Procedure

2.1 Materials

The alumina was an Alcoa XA1000 powder. Figure 1 shows a scanning electron micrograph of the ceramic particles. Note the absence of agglomeration and the complex particle shape. The particle size distribution was determined by sedimentation. The powder consists of fine particles with a mean size near 0·6 μm, with some bigger particles near 2 μm. This distribution is presented in Fig. 2.

The binder was a thermoplastic compound, polystyrene-based. The polymer was mixed with butyl oleate to reduce viscosity and improve wetting of the powder by the binder. The system used in the present study is composed of polystyrene 74% and butyl oleate 26% by weight.

The ceramic–binder compound was prepared with a Z-blade mixer (APV type LXl). Composition was determined by injection moulding tests to achieve the best compromise between debinding time, injectability and sintered parts quality. A compound containing 60% vol Al_2O_3 was chosen. Mixing conditions were fixed to 150°C for 30 min. These conditions were strictly respected for each preparation to avoid differences in flow properties due to the polymer degradation.[1]

2.2 Capillary rheometer

Commercially available rheometers which are often used to characterize powder injection feedstock typically work with shear rates up to a few thousand per second. Powder injection moulding usually encounters shear rates up to 100 000 per second. An apparatus has been designed that allowed measurement of viscosity for a wide range of shear rate, from 10 to 10 000 per second. Such shear rates can be reached through capillary flow. A capillary rheometer allowing work under accurate injection moulding conditions has been developed. This apparatus fits at the end of the

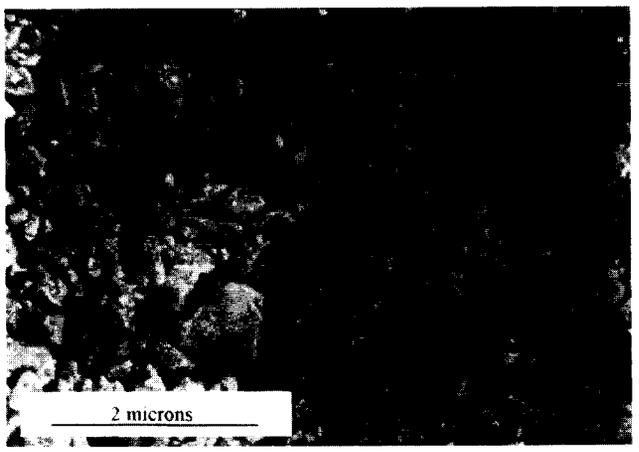

Fig. 1. Scanning electron micrograph of the alumina powder.

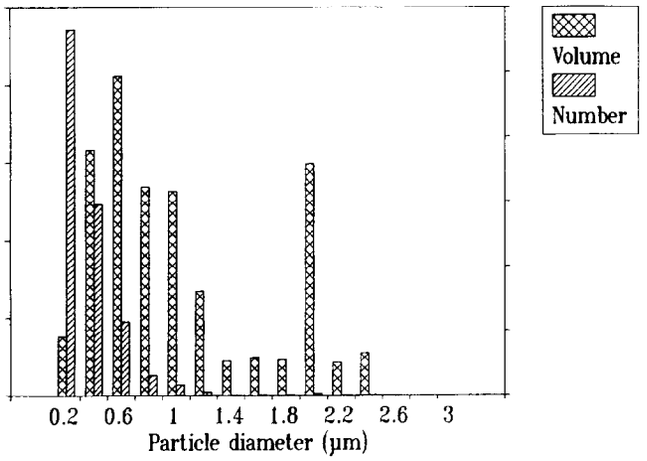

Fig. 2. Particle size distribution of the alumina powder.

injection moulding machine like a mould. According to this principle, rheological measurements take place as a special injection.

The injection moulding machine was an hydraulic screw machine Arburg type Allrounder 221-75-350. It was fitted with four heating zones (heating nozzle) and a hardening treatment of the injection unit (nozzle, screw, barrel and check ring).

Pressure transducers (Dynisco PT435A) were placed at the ends of the capillary to measure the pressure drop. The flow rate is deduced from a LVDT transducer (TNC L50R). The principle of the measurement is shown in Fig. 3. The rheometer was fully thermally regulated and an alumina capillary was used to avoid wear. A wide variety of capillary sizes could be used, ranging from 1 to 7 mm in diameter and 70 to 140 mm in length.

Initially, the capillary rheometer was calibrated with polypropylene supplied by Atochem (Appryl 7228). A good agreement was observed between viscosity measurement and Atochem data. Note that results were not affected by the capillary length. This indicates that viscosity measurement could be used without Bagley's end correction.[2]

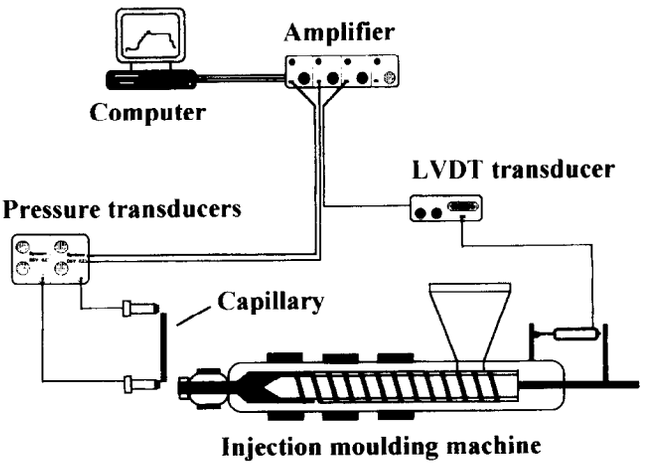

Fig. 3. Principle of the developed capillary rheometer.

3 Results and Discussion

3.1 Viscosity measurements

Viscosity measurements were carried out at temperatures ranging from 160 to 220°C. Three capillary diameters of 2, 5 and 7 mm and several lengths of 70, 115 and 125 mm were tested. Figures 4(a–d) show the wall shear stress versus apparent shear rate for the four temperatures studied. For the sake of simplicity, the rheological curves are presented without Rabinowitsch correction.

The shear rate $\dot{\gamma}$ is expressed as:

$$\dot{\gamma} = \frac{4q}{\pi R^3} \tag{1}$$

and the wall shear stress τ_p is given by:

$$\tau_p = \frac{R\Delta P}{2L} \tag{2}$$

In eqns (1) and (2), R is the capillary radius, L the capillary length, q the flow rate and ΔP the pressure drop.

Three distinct zones could be observed on rheological curves:

On zone 2, the response of the material is dependent on the diameter of the capillary employed. The wall shear stress value decreases with decreasing capillary diameter. This phenomenon was observed for each temperature except for 160°C. This indicates the presence of wall slip at 180, 200 and 220°C.

The decrease of wall shear stress with decreasing capillary diameter is also present in zone 1. In this zone, the wall shear stress becomes independent of the apparent shear rate. For each temperature studied, a critical shear stress value of 0·2 MPa could not be exceeded (zone 3). Beyond this value, the flow stopped whatever the capillary geometry. Moreover, this phenomenon is irreversible. This dilatant behaviour is generally considered to be due to powder separation from the binder.[3]

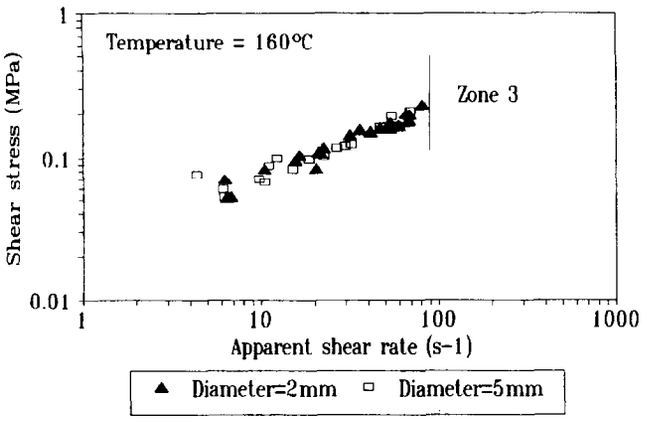

(a)

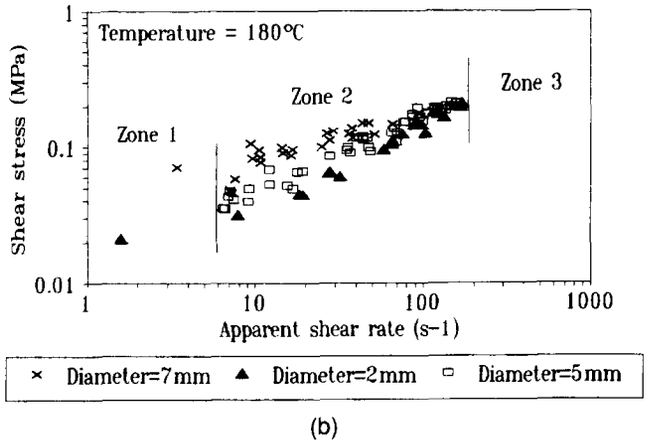

(b)

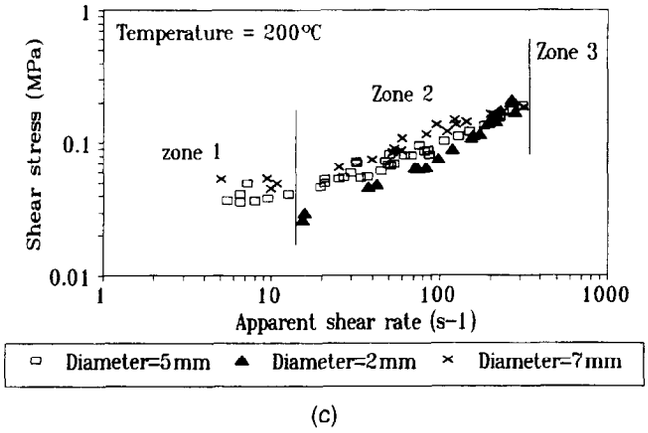

(c)

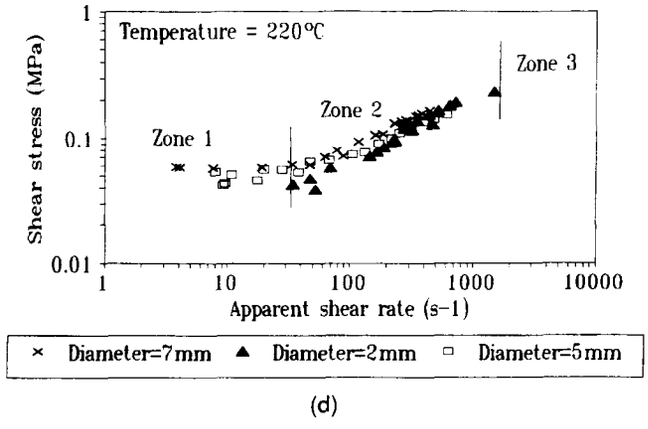

(d)

Fig. 4. Shear stress versus the apparent shear rate from capillary experiments at (a) 160°C; (b) 180°C; (c) 200°C; (d) 220°C.

3.2 Characterization of slip

The wall slip phenomenon was studied using a classical Mooney's method.[4] According to this method, the slip velocity V_s can be determined from the following expression:

$$4V_s = \left.\frac{\partial\left(\frac{4Q}{\pi R^3}\right)}{\partial\left(\frac{1}{R}\right)}\right|_{\tau_w} \tag{3}$$

in which Q and τ_w represent the total volumetric flow rate and wall shear stress, R being the radius of the capillary die. The slip velocity V_s becomes a function of the wall shear stress. It is determined by plotting the apparent shear rate against the reciprocal capillary radius, at a given wall shear stress. In this diagram, the slope of the curves is equal to $4V_s$. Figure 5 illustrates this analysis for the temperature of 200°C.

The values of V_s are of interest to determine the volumetric flow rate due to slip Q_s. Q_s is given by the relation:

$$Q_s = \pi R^2 V_s \tag{4}$$

The ratio Q_s/Q represents the contribution of slip to the overall volumetric flow rate. As V_s, Q_s is a function of the wall shear stress. When Q_s is equal to Q, the suspension slips without being deformed, as a plug. Figure 6 shows the Q_s/Q ratio versus τ_w at the temperature of 200°C and for various capillary diameters. The results indicate that the ratio Q_s/Q increases with decreasing τ_w and approaches unity at low shear stress. This result is obtained for each temperature for which the slip was observed (180, 200 and 220°C)

In consequence, the values of Q_s/Q explain why shear stress becomes independent of the apparent shear rate, as exhibited in zone 1 of Figs 4(b-d). This behaviour is generally associated with the shear thinning nature of the suspension.[5]

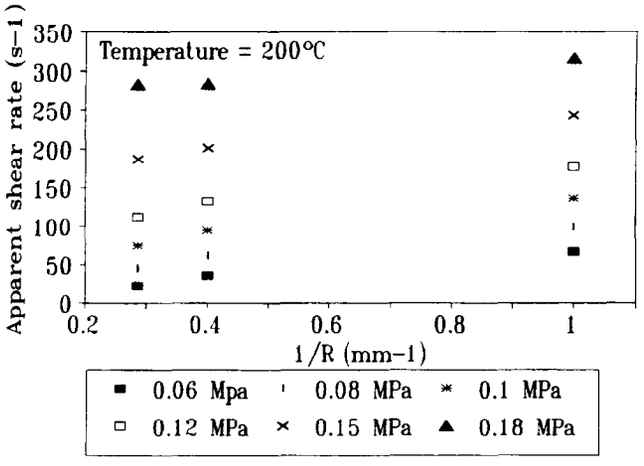

Fig. 5. Mooney's diagram for the calculation of V_s at 200°C.

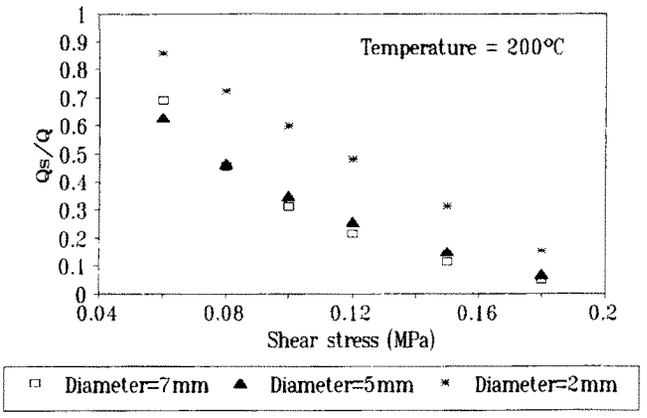

Fig. 6. Q_s/Q values versus the shear stress at the wall for various capillary diameters at 200°C.

Figure 6 shows the importance of wall slip in zone 2. In this zone, the flow rate is due to both slipping and shearing, the greater part of shearing for high shear stress.

All the observed mechanisms can be summarized in a diagram of temperature versus the apparent shear rate (Fig. 7). The zone 4 is deduced from the viscosity measurements at 160°C, where no slip was observed.

The normal or successful mould filling process is characterized by a uniform flow front. In the presence of wall slip, the flow front becomes unsteady, and solid jetting could appear.[6] In consequence, the injection moulding conditions must be provided either in zone 4 or in the low wall slip region of zone 2.

3.3 Origin of slip

The existing studies on apparent slip generally attribute this phenomenon to the formation of a thin polymer fluid layer near the wall of the flow channel as described in Fig. 8. A method to evaluate the slip layer thickness e has been proposed by Cohen.[7] According to this method, e can be determined by the following expression:

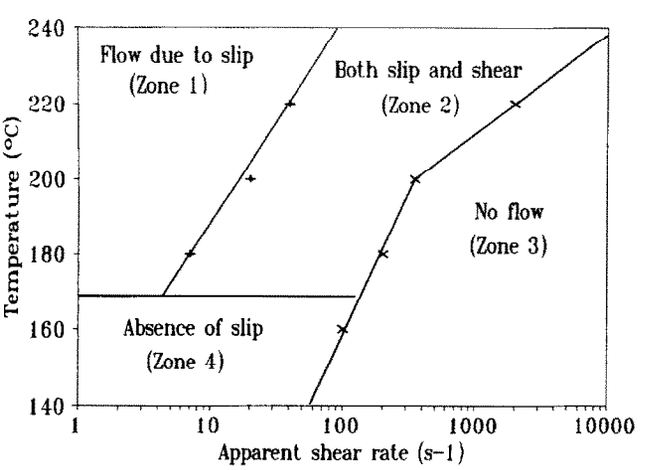

Fig. 7. Behaviour of the alumina suspension studied.

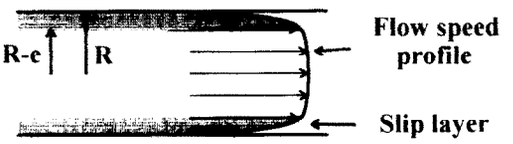

$0 \leq r \leq R\text{-}e$
Layer of high viscosity with low shear stress

$R\text{-}e \leq r \leq R$
Layer of low viscosity with high shear stress

Fig. 8. Schematic representation of a slip layer in a capillary tube.

$$V_s = \frac{1}{2}\left(\frac{e\tau_w}{\eta_w}\right) \tag{3}$$

in which V_s is the slip velocity, η_w represents the viscosity of the slip layer, τ_w being the shear stress at the wall. The expression of v_s described by eqn (3) can be used in the limiting case when the value of e/R is negligible, and the slip layer viscosity is smaller than the fluid viscosity.

In this study, we assume that the slip layer is composed of the binder. Viscosity measurements were carried out on the binder to determine the values of η_w and to verify the absence of wall slip with the binder (Fig. 9). The independence of the flow curves with the capillary radius indicates the absence of the slip phenomenon in the presence of the binder alone. In consequence, the assumption of the presence of a slip layer near the capillary wall as described by Cohen is appropriate to our situation. Moreover, the low binder viscosities are compatible with the expression of e.

It is interesting to compare the rheological behaviour of the ceramic compounds and the binder. The relative viscosity, defined as the relation of the viscosity of the mixture over the viscosity of the pure binder, was found to be strongly dependent on the shear rate. The observed difference, probably due to particle interactions, demonstrates that simple

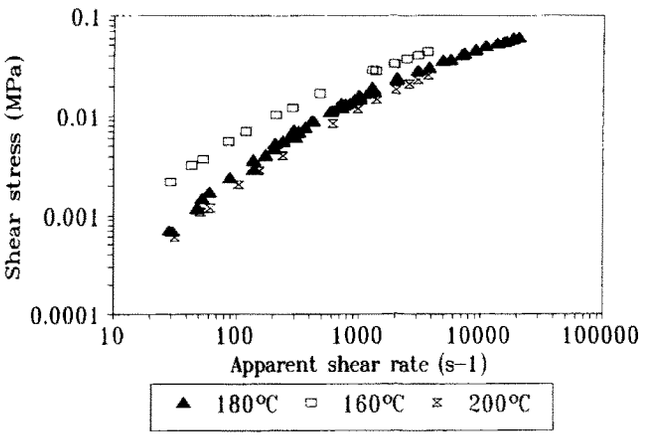

Fig. 9. Rheological behaviour of the binder at 160, 180 and 200°C.

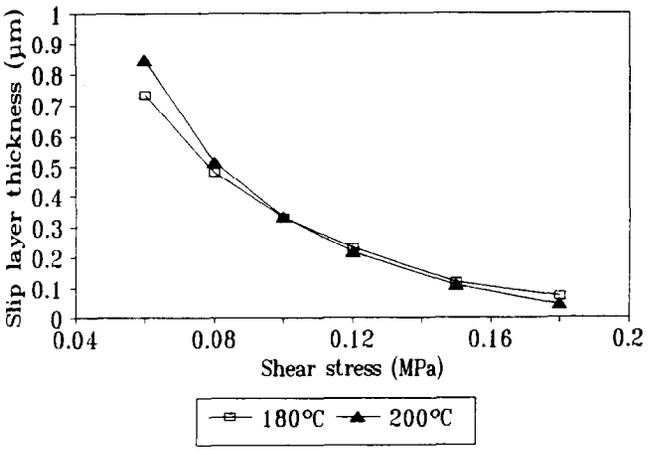

Fig. 10. Slip layer thickness versus wall shear stress at 180 and 200°C.

models as proposed by several authors[8–10] could not predict the rheological behaviour of such a powder–polymer blend, in the sense that they assume a relative viscosity constant for a given volume fraction of filler.

The evolution of this slip layer thickness is shown in Fig. 10. This curve indicates that the decreasing of V_s with increasing wall shear stress can be attributed to the destruction of the slip layer. Note that the calculated slip layer thickness is in the order of magnitude of the mean particle size (near 0·6 μm).

3.4 Comparison with injection moulding tests

Injection moulding tests under several conditions have been performed. The objective was to compare real injection moulding situations with the diagram proposed in Fig. 7. The flow behaviour was studied through interrupted injection. After that, green parts were observed either by X-ray radiography or by direct observation.

Two types of rectangular cavity were used: first, a cavity perpendicular to the gate (mould type A) and, second, a cavity parallel to the gate (mould type B). These two geometries are shown in Figs 11(a) and 11(b).

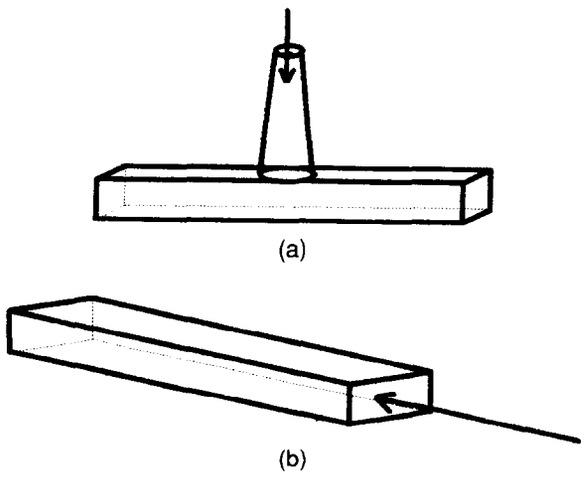

Fig. 11. (a) Cavity perpendicular to the gate (Type A); (b) cavity parallel to the gate (Type B).

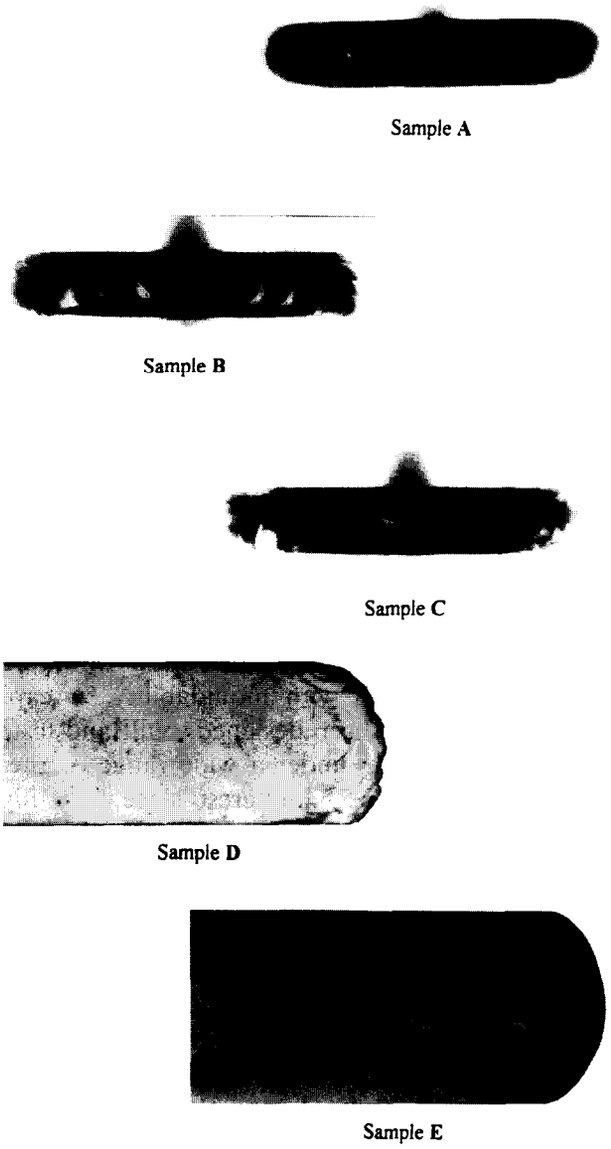

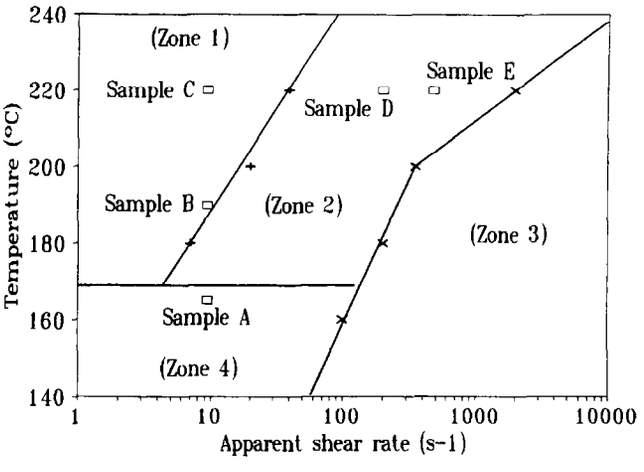

Fig. 12. Injection moulding conditions of samples A to E.

The apparent wall shear rate used for injection moulding tests was estimated using the equation for a rectangular-shaped cavity given by:

$$\dot{\gamma}_w = \frac{6Q}{H^2 L} \quad (4)$$

where Q is the volumetric flow rate, H the short side dimension and L the long side dimension.

The working conditions were chosen so that the various samples lie in zones 1 to 4 (Fig. 12). Samples A, B and C have been achieved with mould A and are X-ray radiographies. Samples D and E are photographs of injections achieved with mould B.

It becomes evident that the unsteady front flow observed on samples B, C and D is the consequence of wall slip. This clearly indicates that the presence of wall slip is correlated with the presence of injection flaws.

4 Conclusion

An attempt was made to correlate laboratory viscosity measurements with mouldability. A capillary rheometer has been designed, built and tested that allows working under a wide range of shear rates. This is of special interest since very high shear rates are often reached in powder injection moulding. Viscosity measurements have been performed on a heavily loaded powder blend using this apparatus. The results obtained on various capillary diameters indicate the presence of wall slip. This phenomenon, which depends on both temperature and shear rate, is responsible for unsteady front flow observed during injection moulding. In consequence, wall slip can be correlated with the presence of injection flaws. Another conclusion is that the rheological behaviour of the mixture could not be simply deduced from the viscosity of the pure binder and from the volume fraction of particles since the relative viscosity depends on the shear rate.

References

1. Hunt, K. N., Evans, J. R. G. & Woodthorpe, J., The influence of mixing route on the properties of ceramic injection moulding blends. *Brit. Ceram. Trans. J.*, **87** (1988) 17–21.
2. Bagley, E. B., End corrections in the capillary flow of polyethylene. *J. Appl. Phys.*, **28** (1957) 624–627.
3. Issit, D. A. & James, P. J., Rheology of mixed powder plastisols. *Powder Metallurgy*, **29** (1986) 259–263.
4. Mooney, M., Explicit formulas for slip and fluidity. *J. Rheol.*, **2**(2) (1931).
5. Kalyon, D. M., Yaras, P., Aral, B. & Yilmazer, U., Rheological behavior of a concentrated suspension: A solid rocket fuel simulant. *J. Rheol.*, **37**(1) (1993) 35–52.
6. Piccirillo, N. & Lee, D., Jetting phenomenon in powder injection moulding. *Int. J. Powder Metallurgy*, **28**(1) (1992) 13–25.
7. Cohen, Y. & Metzner, A. B., Apparent slip flow of polymer solutions. *J. Rheol.*, **29**(1) (1985) 67–102.
8. Frankel, N. A. & Acrivos, A., On the viscosity of a concentrated suspension of solid spheres. *Chem. Eng. Sci.*, **22** (1967) 847–853.
9. Chong, J. S., Christiansen, E. B. & Baer, A. D., Rheology of concentrated suspensions. *J. Appl. Polym. Sci.*, **15** (1971) 2007–2021.
10. Zhang, J. G. & Evans, J. R. G., Predicting the viscosity of ceramic injection moulding suspensions. *J. Eur. Ceram. Soc.*, **5** (1989) 165–172.